journal

J. Am. Ceram. Soc., 91 [12] 3971–3975 (2008)
DOI: 10.1111/j.1551-2916.2008.02782.x

Effect of Thermal Initiator Concentration on the Electrical Behavior of Polymer-Derived Amorphous Silicon Carbonitrides

Yansong Wang,[‡,§] Ligong Zhang,[¶] Weixing Xu,[¶] Tao Jiang,[¶] Yi Fan,[‡] Dapeng Jiang,[‡] and Linan An[*,†,¶]

[‡]Laboratory of Excited State Process, Changchun Institute of Optics, Fine Mechanics and Physics, Chinese Academy of Sciences, Changchun, Jilin 130032, China

[§]Graduate School of Chinese Academy of Sciences, Beijing 100049, China

[¶]Advanced Materials Processing and Analysis Center, University of Central Florida, Orlando, Florida

The electric conductivity of polymer-derived silicon carbonitrides made from a polysilazane modified with different amounts of thermal initiator is measured at room temperature. It is found that the thermal initiator has a significant effect on the electric conductivity, which first increases and then decreases with increasing thermal initiator concentration. The highly conductive sample exhibits a very high piezoresistive coefficient and weak temperature dependence as compared with the low conductive samples. The microstructures of the materials are characterized using a Raman spectroscope. Based on these results, two conducting mechanisms are identified: the highly conductive sample is dominated by the tunneling–percolation mechanism, while the low conductive samples are dominated by matrix phases. The effect of the thermal initiator on the development of the microstructures of the materials is discussed.

I. Introduction

Polymer-derived ceramics (PDCs) are a new class of high-temperature multifunctional materials synthesized by thermal decomposition of polymeric precursors.[1–3] PDCs have attracted considerable attention recently because they exhibit many advantages over traditional ceramics made by powder metallurgy-based processing techniques. For example, the direct chemical-to-ceramic route of PDCs leads to a simple, cost-efficient, and near-net-shape approach to manufacture ceramic components and devices with inconvenient shapes, such as fibers, coatings, composites, and micro-electro-mechanical systems (MEMS)/micro-sensors.[4–9] The technique also offers an opportunity to manipulate the structures and composites, and thereby the properties, of the final ceramics at the atomic/nanoscale by tailoring the chemistry of the precursors. When synthesized at relatively low temperatures (pyrolysis is usually performed at 800°–1000°C), PDCs show excellent high-temperature properties, such as high creep resistance,[10–12] resistance to large-scale crystallization,[2] and excellent oxidation/corrosion resistance.[13–16]

Previous studies on PDCs have primarily been focused on their processing and thermo-mechanical properties. The electrical behavior of the materials has received little attention.[17–20] Previous investigations on PDCs' electrical behavior have found the following phenomena: (i) PDCs possess typical amorphous semiconducting behavior, (ii) the conductivity increases with increasing pyrolysis temperature, (iii) increases in the conductivity seem to coincide with increases in free-carbon concentration, and (iv) the conductivity can be increased by doping. Recently, An and co-workers have also reported that a polymer-derived silicon carbonitride (SiCN) ceramic possesses a significant piezoresistivity with anomalously high gauge factors ranging from 1000 to 4000.[21] They attributed such high gauge factors to the tunneling–percolation network of free-carbon clusters formed in the SiCN. Clearly, a study of the electronic behavior of PDCs is still at its early stage. Further exploration in this direction is highly desired because it could lead to widespread applications of the unique materials in many fields such as for MEMS and micro-sensors, as well as to a fundamental understanding of the property–structure relationships of these interesting materials.

In this paper, we report the effect of thermal initiator concentration on the electrical behavior of polymer-derived amorphous SiCN ceramics. Three kinds of specimens are prepared from a polysilazane precursor that is modified with different amounts of a thermal initiator. We find that electrical properties such as conductivity, temperature-dependent conductivity, and piezoresistivity of the SiCN ceramics can be drastically affected by altering the concentration of the thermal initiator. The results are discussed in terms of the effect of thermal initiator concentration on the microstructures of the materials.

II. Experimental Procedure

The amorphous SiCN ceramics studied here are synthesized by thermal decomposition of a commercially available liquid-phase polysilazane (Ceraset, Kion, Huntingdon Valley, PA) using the technique reported previously.[1,3] Figure 1 shows the chemical structure of Ceraset cited by the supplier[22,23] and confirmed by previous studies.[24,25] A previous study also demonstrated that Ceraset can be converted to SiCN ceramics by thermal decomposition with ~72 wt% yield.[24] To obtain different SiCNs, the precursor is first modified by reacting it with different amounts of dicumyl peroxide (DP) (Table I), which acts as a thermal initiator to lower the solidification temperature of the Ceraset.[24,25] The modified precursors are solidified under different conditions as listed in Table I, followed by heat treatment at 350°C for 4 h in ultra-high-purity nitrogen. The obtained solids are then crushed and ball milled into fine powders using high-energy ball milling. The powders are compressed into disks and then pyrolyzed at 1400°C for 4 h in a tube furnace under flowing of ultra-high-purity nitrogen. The obtained samples are first characterized using XRD, which reveals that the samples obtained are amorphous without any diffraction peak. The compositions of the obtained samples are measured using a combination of elemental analysis and secondary hydrochloric

R. Riedel—contributing editor

Manuscript No. 24576. Received April 22, 2008; approved September 19, 2008.
This work was supported by National Science Foundation of the United States (DMR-0706526).
*Member, The American Ceramic Society.
†Author to whom correspondence should be addressed. e-mail: lan@mail.ucf.edu

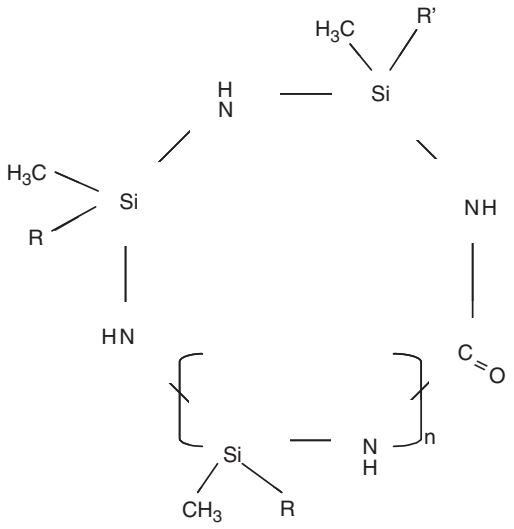

Fig. 1. Chemical structure of Ceraset.

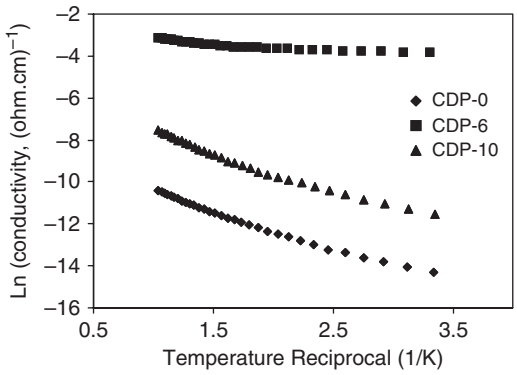

Fig. 2. A plot of the conductivity as a function of temperature for the three samples as indicated in the figure.

acid ICP (Table I). Note that the carbon concentration increases slightly with increasing DP concentration in the precursors.

For characterizing their electrical properties, the obtained specimens are cut into a rectangular shape. A silver paste is painted on the opposite surfaces of the specimens and dried in air for a day to form electrodes. The electrical conductivities of the specimens are measured at room temperature by measuring their current–voltage (*I–V*) curves (Keithley 2400, Keithley instruments Inc., Cleveland, OH). The temperature-dependent conductivities are measured in the temperature range of 25°–700°C using a Digital-Multimeter (UT70C, Uni-Trend Group Limited, Shenzhen, China) by placing specimens in a tube furnace; the measurements are carried out under the flow of ultra-high-purity nitrogen. The stress-dependent resistivities are measured under uniaxial compressive stress at room temperature using the same procedure reported previously.[21]

To characterize the formation of carbon clusters, Raman spectra of the three specimens are obtained using Renishaw in-Via Raman microscope (Renishaw, London, U.K.) with an Ar laser at 514 nm as the excitation source. The lateral resolution of the microscope is 1 cm^{-1}.

III. Results

The room-temperature electrical conductivities of the three specimens are listed in Table I. The results reveal that the conductivities of the SiCNs can be changed drastically by adding DP to their precursor. More significantly, the change in the conductivity is not monotonic with the change of the DP concentration: the conductivity is first increased by about five orders of magnitude from 6.7×10^{-7} to 2.2×10^{-2} $(\Omega \cdot cm)^{-1}$ by adding 6 wt% DP, and then decreased by about four orders of magnitude to 9.1×10^{-6} $(\Omega \cdot cm)^{-1}$ on further increasing the DP concentration to 10 wt%. This last point is very instructive, suggesting that the increase in the conductivity cannot be solely explained by the increase in the carbon concentration due to the DP additives. The form of carbon in the materials could play an important role in determining the conductivity of PDC materials.

The temperature-dependent conductivities of the specimens are plotted in Fig. 2. All three samples exhibit semiconducting behavior with a positive temperature coefficient of the electrical conductivity. The two low-conductivity specimens (CDP-0 and CDP-10) show similar strong temperature-dependent conductivities, while the high-conductivity specimen (CDP-6) shows a much weaker temperature-dependent conductivity. This suggests that CDP-0 and CDP-10 specimens could have the same conducting mechanism, which is different from that for CDP-6.

Figure 3 shows a plot of the resistivity as a function of applied stress for the three specimens. It is seen that all three specimens show positive stress coefficients of electrical resistivity: the resistivity decreases with increasing compressive stress. However, the resistivities of these specimens exhibit different stress-dependent behavior. The high-conductivity CDP-6 specimen shows significant decreases in resistivity as the stress increases, with an ~50% decrease in the resistivity over a stress range of 8 MPa. This behavior is similar to that observed in carbon black–polymer composites.[26–28] On the other hand, the resistivities of the two low conductive CDP-0 and CDP-10 specimens show very weak stress dependence.

The stress dependence of resistivity can be seen more clearly from a piezoresistive stress coefficient, Π, which is defined as

$$\Pi = \frac{d\rho/\rho}{d\sigma} \quad (1)$$

where ρ is the resistivity at the applied stress σ. The piezoresistive stress coefficients of the three specimens are calculated from the data present in Fig. 3 and summarized in Fig. 4. It can be seen that the high-conductivity CDP-6 specimen exhibits a remarkably high piezoresistive stress coefficient, which is much higher than those reported for crystal semiconductors and any ceramic materials.[29–31] It can also be seen that the piezoresistive stress factor of the CDP-6 strongly depends on the applied stress: it decreases by three orders of magnitude from 4 to 0.004 MPa^{-1} over a testing stress range of 8 MPa. On the other hand, the low-conductivity CDP-0 and CDP-10 specimens exhibit much lower piezoresistive coefficients, which also weakly depend on the applied stress. The piezoresistive stress coefficient of

Table I. Precursors, Solidification Conditions, Compositions, and Conductivities of the SiCNs

Sample name	Ceraset-to-DP ratio	Solidification conditions	Compositions	RT conductivity $(\Omega \cdot cm)^{-1}$
CDP-0	100:0	250°C × 2 h	$SiC_{0.97}N_{0.88}O_{0.10}$	6.3×10^{-7}
CDP-6	100:6	150°C × 0.5 h	$SiC_{1.00}N_{0.85}O_{0.11}$	2.2×10^{-2}
CDP-10	100:10	150°C × 0.5 h	$SiC_{1.02}N_{0.83}O_{0.12}$	9.1×10^{-6}

DP, dicumyl peroxide; RT, room temperature, SiCN, silicon carbonitride.

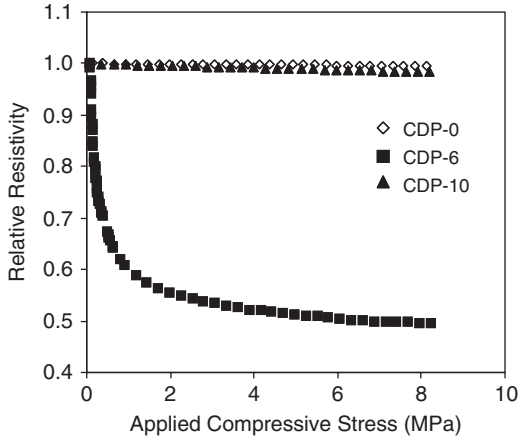

Fig. 3. A plot of the relative resistivities as a function of applied stress for the three specimens as indicated in the figure. The resistivities are normalized with respect to the unstressed value.

the CDP-0 specimen is $\sim 4x10^{-4}$ MPa^{-1}, which is in the same range as that of SiC;[32] and ~ 10 times lower than that of the CDP-10.

The microstructures of the specimens were characterized using a Raman spectroscope. The obtained spectra are presented in Fig. 5. It can be seen that all three spectra show two peaks: *D* and *G* peaks of a graphite phase, suggesting that the SiCNs contain carbon clusters. The *D* peaks for the three specimens are all centered at 1335 cm^{-1}. The *G* peak for CDP-6 is centered at 1544 cm^{-1}, and those for CDP-0 and CDP-10 are centered at 1582 cm^{-1}. These peaks are significantly red shifted as compared with those for free-standing graphite particles, which have *D* and *G* peaks centered at 1355 and 1580 cm^{-1}, respectively.[33] The shifts suggest that there are high residual stresses within the carbon clusters.[34] The figure also reveals that the Raman signal of the CDP-6 is much higher than those of the CDP-0 and CDP-10, suggesting that CDP-6 contains much more carbon clusters than the other two specimens, while the CDP-10 contains only slightly more carbon clusters than the CDP-0. It is surprising that the concentration of the carbon clusters is not monotonically increased with the thermal initiator concentration, even though the total carbon concentration is (see Table I).

The Raman spectra can also be used to estimate the diameter, L_a, of the carbon clusters using the following equation[35]:

$$\frac{I(D)}{I(G)} = \frac{C(\lambda)}{L_a} \tag{2}$$

where $I(D)$ and $I(G)$ are the intensities of *D* and *G* peaks, respectively, and $C(\lambda)$ is a constant that depends on the wavelength of the excitation source. For the excitation source of 515 nm, C is ~ 4.4 nm.[35–38] Based on the spectra shown in Fig. 5, the average diameters of the carbon clusters in CDP-0, CDP-6, and CDP-10 are calculated to be 1.4, 2.0, and 1.7 nm, respectively. This indicates that the diameters of the carbon clusters within the SiCNs are not monotonically changed with the DP concentration: they first increased with the thermal initiator concentration, and then decreased with a further increase in the thermal initiator concentration.

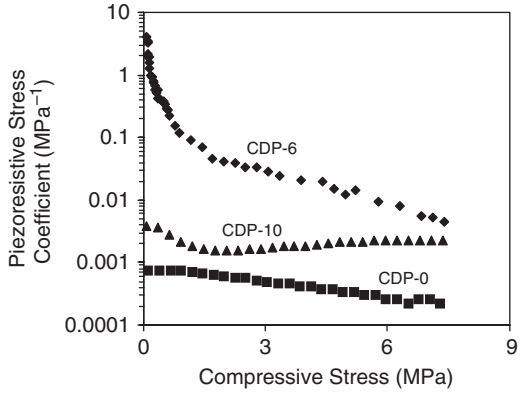

Fig. 4. Piezoresistive stress coefficient of the three samples as a function of applied compressive stress.

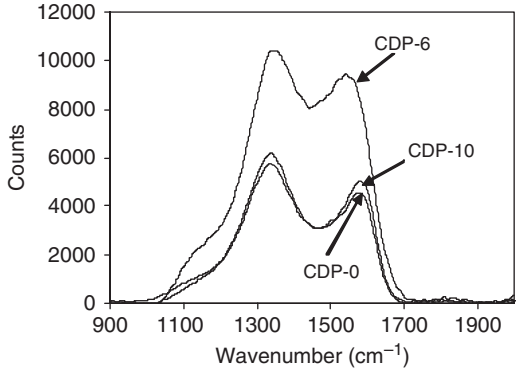

Fig. 5. Raman spectra of samples CDP-0, CDP-6, and CDP-10, as indicated in the figure.

IV. Discussion

An understanding of the electronic behavior of the SiCNs requires detailed information on their microstructures. Unfortunately, such structural information is not accessible experimentally, given the amorphous nature of the materials. Previous studies suggested that PDCs are comprised of an amorphous matrix and distributed carbon clusters (also referred as to free carbons).[19,39,40] For SiCN ceramics, the amorphous matrix is a random network, with SiC_xN_{4-x} ($x = 0$, 1, 2, 3, and 4) being building units, as summarized in Raj *et al.*[41] There are also a fairly high number of C-dangling bonds with unpaired electrons within the matrix due to the loss of hydrogen.[42] Based on this structural model, several conducting mechanisms could function in PDCs, as described schematically in Fig. 6. When the

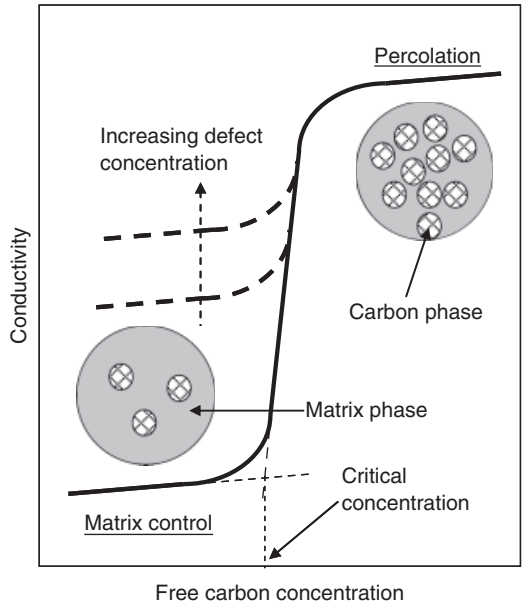

Fig. 6. Schematic showing the possible conducting mechanisms in polymer-derived ceramics.

free-carbon concentration reaches a certain critical level, the electrical conductivity of the material should follow percolation models, while when the carbon concentration is lower than the critical level, the electrical conductivity should be determined by the matrix phase, which should follow amorphous semiconducting behavior.[17,18,43] For the matrix-controlled amorphous semiconducting mechanism, the electrical conductivity is affected by both the chemical bonding configuration of the amorphous network (effect on band gap) and the C-dangling bond concentration (effect on defect concentration).[43]

The results presented in Section III show that the highly conductive CDP-6 also exhibits high piezoresistivity, while the low conductive CDP-0 and CDP-10 show low piezoresistivity. The high piezoresistivity is a clear evidence suggesting that the free-carbon concentration in CDP-6 is high enough to form carbon-cluster-based tunneling–percolation networks and the transport mechanism of the CDP-6 is dominated by the tunneling–percolation process, in which tunneling between the free-carbon clusters coexists with percolation behaviors.[21,44] On the other hand, the CDP-0 and CDP-10 are dominated by the matrix conduction. This is consistent with the Raman results, which reveal that CDP-6 contains much higher free carbons (Fig. 5).

To further demonstrate the transport mechanism of the CDP-6, here we compare the piezoresistivity data with the tunneling–percolation models. According to the previous study,[45] the piezoresistive stress factor of a tunneling–percolation system should have the following stress-dependent relationship:

$$\Pi = \Pi_0 - \alpha \ln\left(\frac{\sigma}{E}\right) + \frac{\beta}{\sigma} \tag{3}$$

where Π_0, α, and β are material-dependent constants,[45] E is the Young's modulus of the material, and σ is the applied stress. Figure 7 plots the piezoresistive stress coefficient data of CDP-6 versus the applied stress. It can be seen that in the low stress range, the data follow log–log dependence (Fig. 7(a)), while in the high stress range the data fit a linear–log relation (Fig. 7(b)), as predicted in Eq. (3). The good agreement between the experimental results and the trends predicted theoretically further confirms that the transport mechanism of the CDP-6 is the tunneling–percolation process.

The transport mechanisms discussed above are also consistent with temperature-dependent conductivity results. It is demonstrated that the tunneling–percolation process leads to a decrease in conductivity with temperature,[26] while the semiconducting process leads to an increase in conductivity. Consequently, the weak temperature-dependent conductivity of the CDP-6 is a combined effect of the two processes, while the strong temperature-dependent conductivities of the CDP-0 and CDP-10 arise from the semiconducting process only.

Now we come to the question as to how the thermal initiator concentration may affect the microstructures of the SiCNs. The clue comes from the solidification processes of the precursor. Without thermal initiator additives, Ceraset is solidified via a reaction between the vinyl groups and C–H bonds (Fig. 1),[24] which occurred at higher temperatures (Table I). When a thermal initiator is added, the solidification of Ceraset is via a radical-induced polymerization process, in which the initiator is first broken into free radicals by thermal energy; the radicals then attack the double bonds of the vinyl groups of Ceraset to start a chain reaction. In such radical-induced polymerization process, which can occur at lower temperatures (Table I), the length of the chains is determined by the concentration of the initiator. The effect of the thermal initiator on the microstructures of the SiCNs can then be understood as follows: for Ceraset without the initiator, all vinyl groups reacted with C–H bonds simultaneously to form very short carbon chains. The carbon clusters are relatively difficult to grow from such short carbon chains. When the proper amount of a thermal initiator is added, the chain reaction can form relatively long carbon chains, which can act as nuclei for further growth of carbon clusters. Therefore, the CDP-6 has larger and more carbon clusters than the CDP-0.

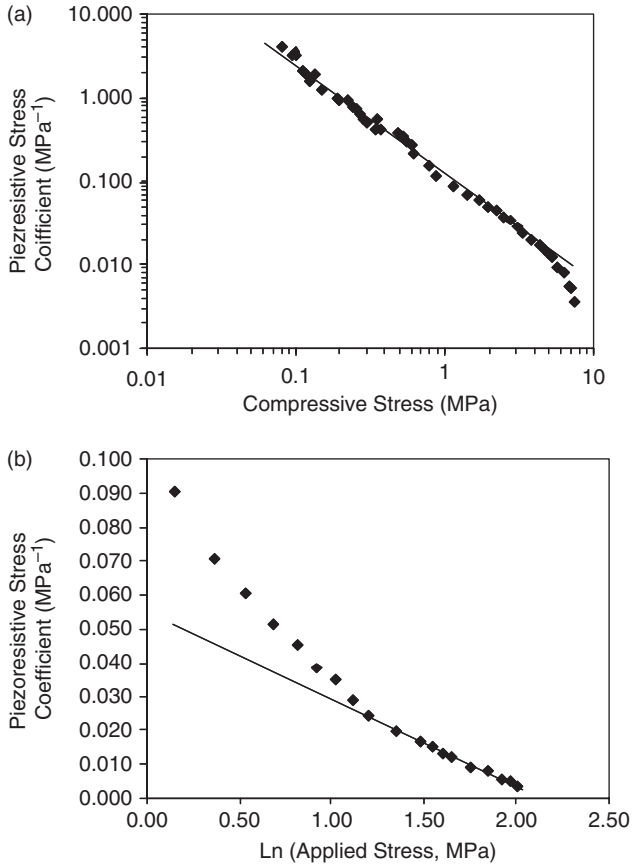

Fig. 7. Piezoresistive stress coefficient of specimen CDP-6 as a function of applied compressive stress: (a) the log–log plot and (b) the linear–log plot. The dots represent the experimental results, while the solid lines are the theoretical trend predicted using Eq. (3).

When the thermal initiator concentration is too high, a large amount of free radicals will be generated simultaneously, which may lead to the formation of short carbon chains. Consequently, a less amount of small free-carbon clusters is formed in CDP-10.

V. Summary

We studied the effect of thermal initiator concentration on the electrical properties of polymer-derived amorphous SiCN ceramics. We demonstrated that the free-carbon concentration, thereby the electrical behavior, of the SiCNs can be controlled by tailoring the concentration of the thermal initiator. The experimental results provide clear evidences that there are two transport mechanisms in the SiCNs: free-carbon-controlled tunneling–percolation and matrix-controlled amorphous semiconducting. The results can also be used as a guideline for developing PDCs with controlled electrical properties.

References

[1]R. Riedel, G. Passing, H. Schonfelder, and R. J. Brook, "Synthesis of Dense Silicon-Based Ceramics at Low-Temperatures," *Nature*, **35**, 714–6 (1992).

[2]R. Riedel, A. Kienzle, W. Dressler, L. Ruwisch, J. Bill, and F. Aldinger, "A Silicoboron Carbonitride Ceramics Stable to 2000 Degrees C," *Nature*, **382**, 796–8 (1996).

[3]E. Kroke, Y. L. Li, C. Konetschny, E. Lecomte, C. Fasel, and R. Riedel, "Silazane Derived Ceramics and Related Materials," *Mater. Sci. Eng. Res.*, **26**, 97–199 (2000).

[4]S. Yajima, Y. Hasegawa, K. Okamura, and T. Matsuzawa, "Development of High-Tensile-Strength Silicon Carbide Fiber Using an Organosilicon Polymer Precursor," *Nature*, **273**, 525–7 (1978).

[5]L. An, W. Xu, S. Rajagopalan, C. Wang, H. Wang, J. Kapat, L. Chow, Y. Fan, L. Zhang, D. Jiang, B. Guo, J. Liang, and R. Vaidyanathan, "Carbon Nanotube Reinforced Polymer-Derived Ceramic Composites," *Adv. Mater.*, **16** [22] 2036–40 (2004).

[6]P. Greil, "Polymer-Derived Engineering Ceramics," *Adv. Eng. Mater.*, **2** [6] 339–48 (2000).
[7]L. Liew, W. Zhang, L. An, S. Shah, R. Lou, Y. Liu, T. Cross, K. Anseth, V. Bright, and R. Raj, "Ceramic MEMS—New Materials, Innovative Processing and Futuristic Applications," *Am. Ceram. Soc. Bull.*, **80** [5] 25–30 (2001).
[8]Y. Liu, L. Liew, R. Lou, L. An, V. M. Bright, M. L. Dunn, J. W. Daily, and R. Raj, "Application of Microforging in SiCN MEMS Structure Fabrication," *Sensors Actuators: A. Physical*, **95** [2–3] 143–51 (2002).
[9]L. Liew, Y. Liu, R. Luo, T. Cross, L. An, V. M. Bright, M. L. Dunn, J. W. Daily, and R. Raj, "Fabrication of SiCN MEMS by Photopolymerization of Pre-Ceramic Polymer," *Sensors Actuators: A. Physical*, **95** [2–3] 120–34 (2002).
[10]L. An, R. Riedel, C. Konetschny, H.-J. Kleebe, and R. Raj, "Newtonian Viscosity of Amorphous Silicon Carbonitride at High Temperature," *J. Am. Ceram. Soc.*, **81**, 1349–52 (1998).
[11]R. Riedel, L. M. Ruwisch, L. An, and R. Raj, "Amorphous Silicoboron Carbonitride Ceramics with Anomalously High Resistance to Creep," *J. Am. Ceram. Soc.*, **81**, 3341–4 (1998).
[12]G. Thum, J. Canel, J. Bill, and F. Aldinger, "Compression Creep Behavior of Precursor-Derived Si–C–N Ceramics," *J. Eur. Ceram. Soc.*, **19**, 2317–23 (1999).
[13]Y. Wang, Y. Fan, L. Zhang, W. Zhang, and L. An, "Polymer-Derived SiAlCN Ceramics Resist to Oxidation at 1400°C," *Scr. Mater.*, **55**, 295–7 (2006).
[14]Y. Wang, W. Fei, Y. Fan, L. Zhang, W. Zhang, and L. An, "A Silicoaluminum Carbonitride Ceramic Resist Oxidation/Corrosion in Water Vapor," *J. Mater. Res.*, **21** [7] 1625–8 (2006).
[15]Y. Wang, Y. Fan, L. Zhang, S. Burton, Z. Gan, and L. An, "Oxidation of Polymer-Derived SiAlCN Ceramics," *J. Am. Ceram. Soc.*, **88** [11] 3075–80 (2005).
[16]L. An, Y. Wang, L. Bharadwaj, Y. Fan, L. Zhang, D. Jiang, Y. Sohn, V. Desai, J. Kapat, and L. Chow, "Silicoaluminum Carbonitride with Anomalously High Resistance to Oxidation and Hot Corrosion," *Adv. Eng. Mater.*, **6** [5] 337–40 (2004).
[17]P. A. Ramakrishnan, Y. T. Wang, D. Balzar, L. An, C. Haluschka, R. Riedel, and A. Herman, "Silicoboron–Carbonitride Ceramics: A Class of High-Temperature, Dopable Electronic Materials," *Appl. Phys. Lett.*, **78** [20] 3076–8 (2001).
[18]A. M. Hermann, Y. T. Wang, P. A. Ramakrishnan, D. Balzar, L. An, C. Haluschka, and R. Riedel, "Structure and Electronic Transport Properties of Si–(B)–C–N Ceramics," *J. Am. Ceram. Soc.*, **84** [10] 2260–4 (2001).
[19]J. Cordelair and P. Greil, "Electrical Conductivity Measurements as a Microprobe for Structure Transitions in Polysiloxane Derived Si–O–C Ceramics," *J. Eur. Ceram. Soc.*, **20**, 1947–57 (2000).
[20]C. Haluschka, C. Engel, and R. Riedel, "Silicon Carbonitride Ceramics Derived from Polysilazanes: Part II. Investigation of Electrical Properties," *J. Eur. Ceram. Soc.*, **20**, 1365–74 (2000).
[21]L. Zhang, Y. Wang, Y. Wei, W. Xu, D. Fang, L. Zhai, K. Lin, and L. An, "A Silicon Carbonitride Ceramic with Anomalously High Piezoresistivity," *J. Am. Ceram. Soc.*, **91**, 1346–9 (2008).
[22] (a)J. M. Schwark, "Isocyanate-Modified Polysilazane Ceramic Precursors," *Polym. Prepr.*, **32**, 567–8 (1991) (b) J. M. Schwark and M. J. Sullivan, "Isocyanate-Modified Polysilazanes: Conversion to Ceramic Materials," *Mater. Res. Soc. Proc.*, **271**, 807–12 (1992).
[23] (a)J. M. Schwark "Organic Amide-Modified Polysilazane Ceramic Precursors," U.S. Patent 5 032 649, 1991. (b) J. M. Schwark, "Isocyanate- and Isothiocyanate-Modified Polysilazane Ceramic Precursors," U.S. Patent 4 929 704, 1991.
[24]Y. Li, E. Kroke, R. Riedel, C. Fasel, C. Gervais, and F. Babonneau, "Thermal Cross-Linking and Pyrolytic Conversion of Poly(ureamethylvinyl)silazanes to Silicon-Based Ceramics," *Appl. Organometal. Chem.*, **15**, 820–32 (2001).
[25]A. Dhamne, W. Xu, B. Fookes, Y. Fan, L. Zhang, S. Burton, J. Hu, J. Ford, and L An, "Polymer–Ceramic Conversion of Liquid Polyaluminasilazanes for SiAlCN Ceramics," *J. Am. Ceram. Soc.*, **88**, 2415–9 (2005).
[26]B. Lundberg and B. Sundqvist, "Resistivity of a Composite Conducting Polymer as a Function of Temperature, Pressure, and Environment: Applications as a Pressure and Gas Concentration Transducer," *J. Appl. Phys.*, **60**, 1074–9 (1986).
[27]F. Carmona, R. Canet, and P. Delhaes, "Piezoresistivity of Heterogeneous Solids," *J. Appl. Phys.*, **61**, 2550–7 (1987).
[28]L. Flandin, A. Hiltner, and E. Baer, "Interrelationship Between Electrical and Mechanical Properties of a Carbon Black-Filled Ethylene–Octene Elastomer," *Polymer*, **42**, 827–38 (2001).
[29]Y. Kanda and K. Suzuki, "Origin of the Shear Piezoresistance Coefficient-PI-44 of *n*-Type Silicon," *Phys. Rev. B*, **43**, 6754–6 (1991).
[30]J. S. Shor, D. Goldstein, and A. D. Kurtz, "Characterization of *n*-Type Beta-SiC as a Piezoresistor," *IEEE Trans. Elect. Devices*, **40**, 1093–9 (1993).
[31]T. Toriyama and S. Sugiyama, "Analysis of Piezoresistance in *n*-Type Beta-SiC for High-Temperature Mechanical Sensors," *Appl. Phys. Lett.*, **81**, 2797–9 (2002).
[32]M. Eickhoff, M. Moller, G. Kroetz, and M. Stutzmann, "Piezoresistive Properties of Single Crystalline, Polycrystalline, and Nanocrystalline *n*-type 3C-SiC," *J. Appl. Phys.*, **96**, 2872–7 (2004).
[33]S. Reich and C. Thomsen, "Raman Spectroscopy of Graphite," *Philos. Trans. R. Soc. Lond. A*, **362**, 2271–88 (2004).
[34]T. Cross, R. Raj, S. V. Prasad, T. E. Buchheit, and D. R. Tallant, "Mechanical and Tribological Behavior of Polymer-Derived Ceramics Constituted from $SiC_xO_yN_z$," *J. Am. Ceram. Soc.*, **89**, 3706–14 (2006).
[35]F. Tuinstra and J. L. Koening, "Raman Spectra of Graphite," *J. Chem. Phys.*, **53**, 1126–30 (1970).
[36]A. C. Ferrari and J. Robertson, "Interpretation of Raman Spectra of Disordered and Amorphous Carbon," *Phys. Rev. B*, **61**, 14095 (2000).
[37]D. S. Knight and W. B. White, "Characterization of Diamond Films by Raman Spectroscopy," *J. Mater. Res.*, **4**, 385–93 (1989).
[38]M. J. Mathews, M. A. Pimenta, G. Dresselhaus, M. S. Dresselhaus, and M. Endo, "Origin of Dispersive Effects of the Raman *D* Band in Carbon Materials," *Phys. Rev. B*, **59**, R6585–8 (1999).
[39]A. Saha, R. Raj, and D. L. Williamson, "A Model for the Nanodomains in Polymer-Derived SiCO," *J. Am. Ceram. Soc.*, **89**, 2188–98 (2006).
[40]A. Saha, R. Raj, D. L. Williamson, and H. K. Kleebe, "Characterization of Nanodomains in Polymer-Derived SiCN Ceramics Employing Multiple Techniques," *J. Am. Ceram. Soc.*, **88**, 232–4 (2005).
[41]R. Raj, R. Riedel, and G. Soraru, "Introduction to the Special Topical Issue on Ultrahigh-Temperature Polymer-Derived Ceramics," *J. Am. Ceram. Soc.*, **84**, 2158–9 (2001).
[42]C. Haluschka, H.-J. Kleebe, R. Franke, and R. Riedel, "Silicon Carbonitride Ceramics Derived from Polysilazanes: Part I. Investigation of Compositional and Structural Properties," *J. Eur. Ceram. Soc.*, **20**, 1355–64 (2000).
[43]Y. Wang, T. Jiang, L. Zhang, Y. Fan, D. Jiang, and L. An, "Electron Transport in Polymer-Derived Amorphous Silicon Carbonitrides," *Appl. Phys. Lett.*, in review.
[44]S. Vionnet-Menot, C. Grimaldi, T. Maeder, S. Strassler, and P. Ryser, "Tunneling-Percolation Origin of Nonuniversality: Theory and Experiments," *Phys. Rev. B*, **71**, 064201–12 (2005).
[45]Y. Wang, L. Zhang, Y. Fan, D. Jiang, and L. An, "Stress-Dependent Piezoresistivity in Tunneling–Percolation Systems," *Comp. Part A: Appl. Sci.*, in review. □